Equivalent retarder-rotator approach to on-state twisted nematic liquid crystal displays

Vicente Durán, Jesús Lancis, Enrique Tajahuerce, and Zbigniew Jaroszewicz

Citation: Journal of Applied Physics **99**, 113101 (2006); doi: 10.1063/1.2198929
View online: http://dx.doi.org/10.1063/1.2198929
View Table of Contents: http://scitation.aip.org/content/aip/journal/jap/99/11?ver=pdfcov
Published by the AIP Publishing

Equivalent retarder-rotator approach to on-state twisted nematic liquid crystal displays

Vicente Durán, Jesús Lancis,[a] and Enrique Tajahuerce
Department de Ciències Experimentals, Universitat Jaume I, 12080 Castelló, Spain

Zbigniew Jaroszewicz
Department of Physical Optics, Institute of Applied Optics, Warsaw 03-805, Poland

(Received 16 June 2005; accepted 29 March 2006; published online 1 June 2006)

Polarization properties of a twisted nematic liquid crystal cell are fully characterized by an equivalent optical system that consists of a retarder wave plate and a rotator. In this paper we show that this result is of interest to optimize the light-modulation capabilities of a voltage-addressed liquid crystal display (LCD). We provide two examples. First, we demonstrate a calibration method that can be carried out by a standard polarimetric technique with a high degree of precision. Second, we propose an optical device to generate a family of equiazimuth polarization states by adding a quarter-wave plate to the LCD. We find that the design procedure is best described in geometrical terms on the Poincaré sphere by use of the equivalent model. Finally, laboratory results corresponding to a commercial LCD are presented. © *2006 American Institute of Physics*.
[DOI: 10.1063/1.2198929]

I. INTRODUCTION

Twisted nematic liquid crystal displays (TNLCDs) are optoelectronic pixilated devices that can act as programable spatial light modulators (SLMs) for coherent optical signal processing operations. Every pixel contains a thin liquid crystal layer with twist molecular alignment and is coated with transparent electrodes. This makes it possible to apply an electric field across the cell to tilt the molecules. In order to optimize the modulation response of a TNLCD, a reliable model to describe the molecular behavior in the on state is required. A numerical method for computing the change in molecular orientation was proposed by Berreman.[1] Lu and Saleh presented a simplified mathematical model based on the Jones matrix formulation.[2] They assumed that molecules twist linearly along the cell gap and have a constant tilt for each value of the applied voltage. In this case, an analytical solution for the Jones matrix of the liquid crystal cell can be obtained. However, the assumptions of the Lu and Saleh approach do not hold for the current flat commercial TNLCDs. For this reason several improvements of this model have been reported in the last few years.[3,4] From an experimental point of view, the Jones matrix of the cell has been determined for every value of the applied voltage by seven nonstandard irradiance measurements.[5] After that, the light-modulation capabilities of the LCD have been evaluated numerically.

Based on the fact that any phase shifter is entirely equivalent to a system consisting of a retarder followed by a rotator,[6–8] the design parameters of an off-state cell, which are the twist angle, the twist sense, the retardation, and the rubbing direction, have been obtained for both a reflective[9] and a transmissive[10] LCD. Within the above framework, the aim of this paper is twofold. First, we extend the equivalent-system approach to deal with a voltage-addressed LCD. We find that this model provides a convenient geometrical description of the light-modulation capabilities of a liquid crystal cell in terms of two simple rotations on the Poincaré sphere. And second, the practical interest of the proposed approach is highlighted in two applications related to the design of polarization devices: an original calibration technique for a LCD and the design of an equiazimuth polarization state (EAPS) generator. Concerning the first application, we propose cell calibration with circularly polarized light by measuring the Stokes parameters of the transmitted light. As a main advantage with respect to the calibration procedure outlined in Ref. 5, only standard polarimetric quantities (the Stokes parameters) are employed. As a result, the method benefits from the high precision of commercially available Stokesmeters. The accuracy of the proposal is another practical benefit to be taken into account. The second application is the generation of a family of EAPSs, which constitutes a major challenge in the field of ellipsometry.[11] As a matter of fact, they have been recently employed for the identification of polarization singularities of arbitrary vector fields[12] by means of interferometric methods.[13] With regard to spatial light modulation, EAPSs provide an efficient way to generate a voltage controlled phase shift without altering the amplitude of the incident light wave.[14]

This article has been organized as follows. In Sec. II, after a review of the equivalent model to describe the optical behavior of TNLCDs, the calibration procedure is outlined. We prove that the parameters of the equivalent system, which are the phase shift and the rotation angle, can be easily evaluated. This can be done by measuring the Stokes parameters of the output light beam when the liquid crystal cells are illuminated with circularly polarized light. In this way, calibration curves for the equivalent parameters as a function of the addressed gray level are presented for a commercially available TNLCD. Also, the precision of the technique is

[a]Electronic mail: jesus.lancis@exp.uji.es

evaluated by means of rigorous error analysis. In Sec. III, the retarder-rotator approach is used to search for an EAPS generator. We show that a TNLCD inserted between an input polarizer and an output quarter-wave plate can generate a family of EAPSs. The optimal angles of the polarization elements are found with the aid of the Jones calculus. The solutions obtained by numerical calculations admit a geometrical interpretation on the Poincaré sphere. The validity of this configuration is verified experimentally for the aforementioned display and shows the practical interest of the model. Finally, conclusions are summarized in Sec. IV.

II. CALIBRATION PROCEDURE

A. Equivalent parameter model

Let us begin by recalling that the Jones matrix of a twisted nematic liquid crystal cell, $\mathbf{M}_{\mathrm{TNLCD}}$, referred to a frame with the x axis in the direction of the input molecular director (liquid crystal framework), is given by[15]

$$\mathbf{M}_{\mathrm{TNLCD}} = \exp(-i\beta)\mathbf{R}(-\phi)\mathbf{U}(\phi,\beta). \tag{1}$$

In the above equation the symbols ϕ and β stand, respectively, for the molecular twist and the birefringence. Furthermore, $\mathbf{R}(\cdot)$ is the rotation matrix and $\mathbf{U}(\phi,\beta)$ is a well-known unimodular unitary matrix that depends on the design parameters ϕ and β.

Next, we employ the fact that any unitary matrix $\mathbf{U}$ has an optically equivalent system consisting of one retardation plate and one rotator.[6] In mathematical terms,

$$\mathbf{U} = \mathbf{R}(\omega_{\mathrm{eq}})\mathbf{WP}(2\delta_{\mathrm{eq}}, \theta_{\mathrm{eq}}), \tag{2}$$

where $\mathbf{WP}(2\delta_{\mathrm{eq}}, \theta_{\mathrm{eq}})$ is the Jones matrix of a retardation plate whose phase difference between the slow and the fast eigenstates is equal to $2\delta_{\mathrm{eq}}$ and whose slow axis has the angle θ_{eq} with the x axis. In Eq. (2), $\mathbf{R}(\omega_{\mathrm{eq}})$ denotes the Jones matrix of a rotator of angle ω_{eq}. We note that the order of the matrix product in Eq. (2) can be reversed; i.e., the opposite sequence of polarization elements is also possible. In this case, the value of the equivalent parameters changes as long as the association of a retarder and a rotator is not symmetrical.

A deeper insight into the modulation capabilities of the cell is obtained when $\mathbf{M}_{\mathrm{TNLCD}}$ is written in terms of the equivalent-model parameters rather than in terms of the design parameters ϕ and β. With this aim, by taking into account Eq. (2) and the fact that for a TNLCD $\theta_{\mathrm{eq}} = \omega_{\mathrm{eq}}/2$,[10] Eq. (1) is rewritten as

$$\mathbf{M}_{\mathrm{TNLCD}} = \exp(-i\beta)\mathbf{R}(\phi_{\mathrm{eq}})\mathbf{WP}\left(2\delta_{\mathrm{eq}}, \frac{\phi+\phi_{\mathrm{eq}}}{2}\right), \tag{3}$$

where $\phi_{\mathrm{eq}} = -\phi + \omega_{\mathrm{eq}}$. Note that the composition rule $\mathbf{R}(\varepsilon)\mathbf{R}(\sigma) = \mathbf{R}(\varepsilon+\sigma)$ for rotation matrices has been applied in order to write Eq. (3). Once the molecular twist ϕ is known and aside from a global phase shift, the twisted nematic liquid crystal cell is fully characterized by the two equivalent parameters δ_{eq} and ϕ_{eq}. Although the above choice of parameters is not unique, we claim that it is a convenient one, as they are independent of the coordinate framework.

The equivalent retarder-rotator model is valid both for an off state and an addressed state provided that the voltage-induced molecular redistribution does not involve any light attenuation. Note that equivalent parameters depend on the applied voltage (or the addressed gray level g in the case of a commercial TNLCD). Next, an experimental procedure to determine the curves $\delta_{\mathrm{eq}}(g)$ and $\phi_{\mathrm{eq}}(g)$ is developed.

B. Equivalent parameter measurement

As we show next, a simple calibration procedure involves the illumination of the TNLCD with circularly polarized light and the determination of the transmitted polarization state by means of Stokes parameter measurement. For right-handed circularly polarized light, the output normalized Jones vector, in the liquid crystal framework, can be obtained as the matrix product,

$$\begin{pmatrix} E_x \\ E_y \end{pmatrix} = \exp(-i\beta)\mathbf{R}(\phi_{\mathrm{eq}})\mathbf{WP}\left(2\delta_{\mathrm{eq}}, \frac{\phi+\phi_{\mathrm{eq}}}{2}\right)\begin{pmatrix} 1 \\ i \end{pmatrix}. \tag{4}$$

The Stokes parameters for the emerging light can be derived by the following expressions:[11]

$$\begin{aligned} S_0 &= E_x E_x^* + E_y E_y^* = 1, \\ S_1 &= E_x E_x^* - E_y E_y^*, \\ S_2 &= E_x E_y^* + E_x^* E_y, \\ S_3 &= i(E_x E_y^* - E_x^* E_y), \end{aligned} \tag{5}$$

where the symbol * indicates the complex conjugate. Taking into account the Jones matrix of the association of a retarder and a rotator,[6] substituting E_x and E_y calculated in accordance with Eq. (4) into Eq. (5), and after some straightforward algebraical manipulations, we obtain

$$\begin{aligned} S_0 &= 1, \\ S_1 &= \sin(\phi - \phi_{\mathrm{eq}})\sin 2\delta_{\mathrm{eq}}, \\ S_2 &= -\cos(\phi - \phi_{\mathrm{eq}})\sin 2\delta_{\mathrm{eq}}, \\ S_3 &= \cos 2\delta_{\mathrm{eq}}. \end{aligned} \tag{6}$$

Two findings are clear from Eq. (6). On one hand, the equivalent phase retardation δ_{eq} can be determined from the experimental measurement of the Stokes parameter S_3, namely,

$$\delta_{\mathrm{eq}} = \tfrac{1}{2}\arccos(S_3). \tag{7}$$

On the other hand, the experimental value of the ratio, S_1/S_2, for which the dependence with δ_{eq} vanishes, allows us to obtain the equivalent rotation angle ϕ_{eq}. In mathematical terms,

$$\phi_{\mathrm{eq}} = \phi + \arctan\left(\frac{S_1}{S_2}\right). \tag{8}$$

Stokes parameters of the light transmitted by the TNLCD can be measured following the operational definitions of S_1, S_2, and S_3 as the difference between normalized

irradiances transmitted by two orthogonal polarizers.[16] Thus, the determination of the equivalent parameters implies the measurement of the following seven intensities obtained from the radiation transmitted through the TNLCD: I_0, the total intensity; $I_{x,y}$, the intensity of the linear components along the x axis and the y axis, respectively; $I_{\pm 45^\circ}$, the intensity transmitted through a linear polarizer oriented at $\pm 45^\circ$ with respect to the x axis; and, finally, $I_{R,L}$, the intensity transmitted through a right-handed and a left-handed circular polarizer. Aside from a normalization factor, Eq. (7) indicates that δ_{eq} is connected with $I_{R,L}$, whereas the equivalent rotation angle is connected with $I_{x,y}$ and $I_{\pm 45^\circ}$. From an experimental point of view, we note that a linear polarizer and a quarter-wave plate are enough to perform the above set of intensity measurements. Once the Stokes parameters are measured for each value of the addressed gray level, calibration curves $\delta_{\mathrm{eq}}(g)$ and $\phi_{\mathrm{eq}}(g)$ can be obtained through Eqs. (7) and (8).

C. Analysis on the Poincaré sphere

A deeper physical insight can be gained at this point if the calibration procedure is interpreted in geometrical terms with the aid of the Poincaré sphere. With this aim, the polarization ellipse of the emerging light is characterized through its ellipticity angle ε and through the inclination of the major axis of the ellipse (the azimuth angle) α, rather than in terms of the Stokes parameters. It is a well-known fact that the vector of components (S_1, S_2, S_3) defines a point on the Poincaré sphere whose spherical coordinates are $(1, 2\alpha, 2\varepsilon)$. In mathematical terms,

$$\varepsilon = \tfrac{1}{2} \arcsin(S_3) \tag{9}$$

and

$$\alpha = \frac{1}{2} \arctan\left(\frac{S_2}{S_1}\right). \tag{10}$$

By substituting Eqs. (7) and (8) into Eqs. (9) and (10), respectively, we obtain the expressions that link the equivalent parameters with the spherical coordinates of the emerging polarization state. In this way, we obtain

$$2\delta_{\mathrm{eq}} = \frac{\pi}{2} - 2\varepsilon \tag{11}$$

and

$$\phi_{\mathrm{eq}} = \frac{\pi}{2} - (2\alpha - \phi). \tag{12}$$

From Eq. (11) we can infer that the polar angle of the output polarization state is solely connected with the equivalent phase retardation δ_{eq}, whereas it does not depend on the equivalent rotation angle ϕ_{eq}. In his turn, ϕ_{eq}, which results independent of δ_{eq}, is determined exclusively by the azimuth of the output, as is shown in Eq. (12). It is important to recognize that the above facts are a result of the choice of a circularly polarized state as input light beam.

Figure 1 illustrates the geometrical interpretation of the action of the TNLCD over an input polarization state on the Poincaré sphere. The initial state $\mathcal{A}$ corresponds to circularly polarized light. The action of the equivalent retarder on $\mathcal{A}$ is just a rotation of angle $2\delta_{\mathrm{eq}}$ along the meridian circle orthogonal to the fast axis of the retarder to the intermediate state $\mathcal{B}$. Finally, a rotation of angle $2\phi_{\mathrm{eq}}$ along the parallel circle determines the output state $\mathcal{C}$.

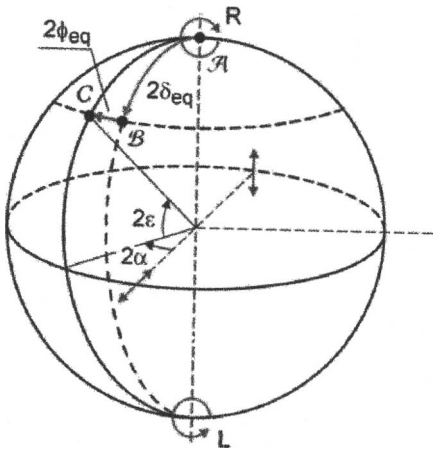

FIG. 1. Action of the TNLCD over an input circularly polarized light on the Poincaré sphere. R and L represent, respectively, right-handed and left-handed circularly polarized states. The angles 2α and 2ε are the spherical coordinates (longitude and latitude) of the output polarization state.

D. Experimental procedure

With the theoretical foundation just given, we measured the calibration curves of a commercial display (Sony LCX016AL with 832×624 32 μm sized pixels). The molecular twist and the maximum birefringence in the off state for the above display were derived by us in a previous paper, obtaining the values $\phi = -1.594$ rad and $\beta_{\max} = 2.255$ rad at $\lambda = 632$ nm.[10] We also found the angle Ψ_D between the input molecular director and the laboratory horizontal axis, $\Psi_D = 2.363$ rad, which fixes the orientation of the liquid crystal framework. The experimental setup is shown in Fig. 2. The TNLCD was illumined with a linearly polarized argon ion laser ($\lambda = 514$ nm). A right-handed circularly polarized light beam was generated with a zero-order quarter-wave plate (Melles Griot 02WRQ011). The Stokes parameters were measured for each gray level from $g = 0$ to $g = 255$ in eight-level steps. To estimate the experimental uncertainty in Stokes parameter values, we repeated the measurements in at

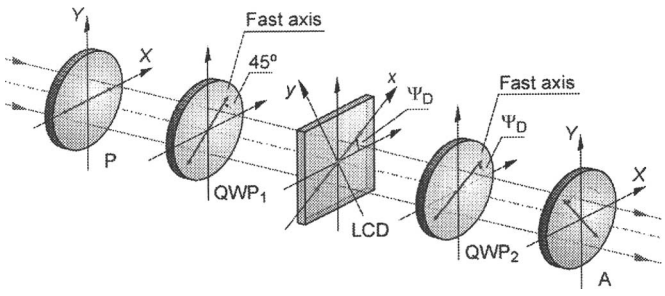

FIG. 2. Experimental setup for equivalent parameter measurement. P is the polarizer; QWP_1, the quarter-wave plate used to generate circularly polarized light; LCD, the sample display; QWP_2, the quarter-wave plate required to measure S_3; A, the analyzer; and Ψ_D, the orientation of the input molecular director with respect to the laboratory horizontal axis.

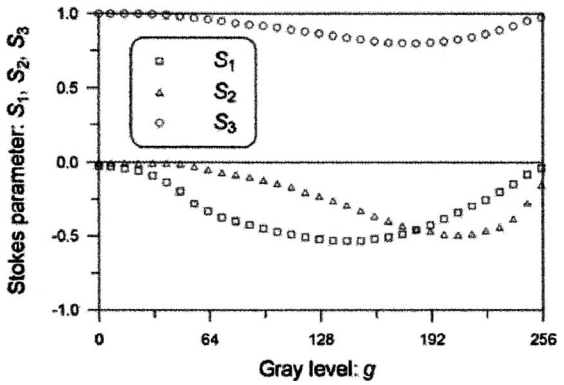

FIG. 3. Experimental results for the Stokes parameters S_1, S_2, and S_3 of the light transmitted by the TNLCD illuminated with right-handed circularly polarized light.

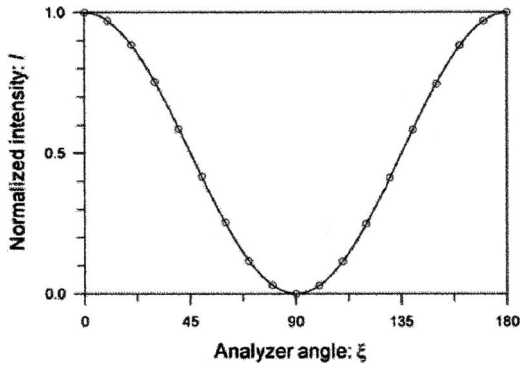

FIG. 4. Transmitted intensity through the TNLCD inserted between an input polarizer and an output analyzer as a function of the analyzer angle for the addressed gray level $g=0$. Measured values of the transmitted intensity are represented with dots and the nonlinear fit with solid line.

least three independent series and no discrepancy greater than ±0.03 was observed for any gray level. This value can be reduced in an order of magnitude by using a commercially available Stokesmeter. Figure 3 shows the evolution of the Stokes parameters S_1, S_2, and S_3 versus gray level.

Now, the corresponding values for the equivalent parameters can be derived from the above set of data by using Eqs. (7) and (8). At this point, standard error propagation techniques must be used in order to determine the precision of the equivalent parameter ϕ_{eq}.[17] In mathematical terms, if the estimated uncertainties of the Stokes parameters S_1 and S_2 are, respectively, σ_1 and σ_2, the corresponding uncertainty for ϕ_{eq} is given by

$$\sigma_{\phi_{\mathrm{eq}}} = \frac{1}{S_1^2 + S_2^2}\sqrt{S_2^2\sigma_1^2 + S_1^2\sigma_2^2}, \tag{13}$$

as can be derived with the usual propagation formula and Eqs. (7) and (8).

Note that, according to Eq. (13), the uncertainty in ϕ_{eq} grows unbounded for light becoming circularly polarized. This situation is observed for low addressed gray levels (see Fig. 3), for which the cell does not change appreciably the input polarization state and therefore the output beam is roughly circularly polarized. Therefore, the precise determination of ϕ_{eq} for low gray levels requires the use of an input polarization state other than circular, which implies a greater calculus complexity. In particular, we have measured the transmitted intensity when the cell is illuminated with linearly polarized light in the direction of the input molecular director and the analyzer is rotated. For this case, the output Jones vector, expressed in the analyzer framework, is given by

$$\begin{pmatrix} E_x \\ E_y \end{pmatrix} = \mathbf{PR}(\xi)\exp(-i\beta)\mathbf{R}(\phi_{\mathrm{eq}})\mathbf{WP}\left(2\delta_{\mathrm{eq}}, \frac{\phi+\phi_{\mathrm{eq}}}{2}\right)\begin{pmatrix} 1 \\ 0 \end{pmatrix}, \tag{14}$$

where ξ is the angle of the analyzer and $\mathbf{P}$ is the matrix of a polarizer with its axis in the x direction. In this way, the normalized intensity transmitted is found to be

$$T = \begin{pmatrix} E_x \\ E_y \end{pmatrix}(E_x^* \; E_y^*)$$
$$= \cos^2\delta_{\mathrm{eq}}\cos^2(\xi+\phi_{\mathrm{eq}}) + \sin^2\delta_{\mathrm{eq}}\cos^2(\xi-\phi). \tag{15}$$

From Eq. (15) a nonlinear curve fitting can be used to determine with high precision the value of ϕ_{eq}. As a by-product, the equivalent retardation angle δ_{eq} is also obtained from the fit. Figure 4 shows the experimental result for the gray level $g=0$, together with the curve obtained by the nonlinear fit. Of course, the outlined procedure is time consuming and the mathematical complexity is greater than using Eqs. (7) and (8). Thus, it was only employed for the first seven gray levels where Eq. (8) provides a nonprecise determination of ϕ_{eq}.

The final calibration curves $\delta_{\mathrm{eq}}(g)$ and $\phi_{\mathrm{eq}}(g)$ are represented in Fig. 5. As is expected, for low values of the gray level, both $\delta_{\mathrm{eq}}(g)$ and $\phi_{\mathrm{eq}}(g)$ are close to zero. Notice that $\delta_{\mathrm{eq}}(g)$ shows, despite a saturation zone at low gray levels, a roughly symmetrical behavior around a local maximum located at $g=175$. Concerning the equivalent rotation angle, it exhibits a monotonic decreasing behavior with the gray scale, reaching at $g=255$ its minimum value.

III. EQUIAZIMUTH POLARIZATION STATE GENERATOR

As stated above, it is clear that for any input polarization state the TNLCD maps the addressed gray level g into a

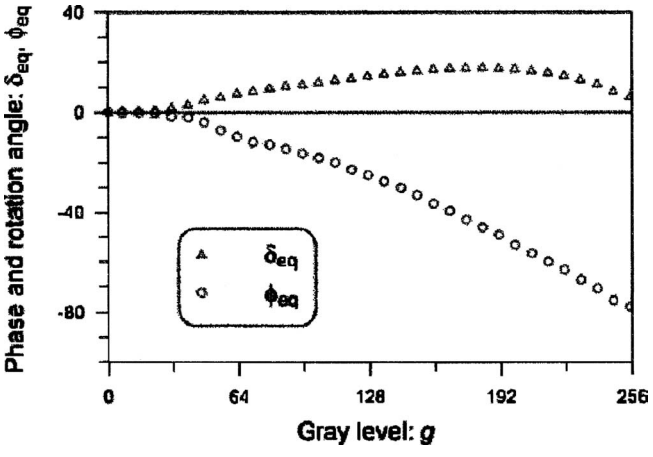

FIG. 5. Representation of measured equivalent parameters δ_{eq} and ϕ_{eq} as a function of the addressed gray level g.

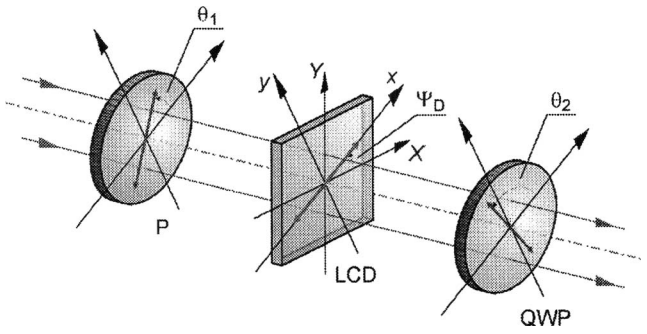

FIG. 6. Experimental setup for generating a set of EAPSs. *P* is the polarizer; LCD, the sample display; QWP, the quarter-wave plate; and θ_1 and θ_2 are, respectively, the polarizer and quarter-wave plate axis angles with respect to the input molecular director of the LCD.

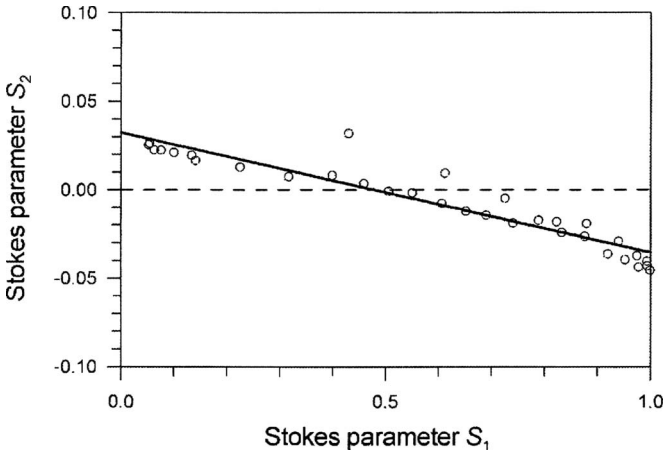

FIG. 7. Representation of the final polarization states on the S_1-S_2 plane for the configuration that provides a set of EAPSs. The solid line is the least-square fit.

polarization ellipse. Next, we face the problem of generating a family of polarization states, each one corresponding to a value of g, with the same direction for the polarization ellipse axes. Although the generation of these equiazimuth states is important in its own right, as mentioned in Sec. I, they give also the opportunity to use the TNLCD as a phase-mostly optical modulator.[14]

First, we provide a heuristic approach to the generation of EAPSs based on the equivalent parameter model and the Poincaré sphere. We begin by considering the action of the cell over a linearly polarized input light beam with its vibration direction at an angle θ_1 with respect to the input molecular director. Initially, the incident state is rotated by the equivalent retarder through an angle $2\delta_{\mathrm{eq}}$ about the plate fast axis.[18] Then, the intermediate elliptically polarized state experiences pure optical rotation due to the action of the equivalent rotor. This results in a final state with the same ellipticity, but with a different azimuth by an amount $2\phi_{\mathrm{eq}}$. The behavior of the equivalent parameters, δ_{eq} and ϕ_{eq}, in Fig. 5, allows us to figure out that the output polarization states will approximately trace the arc of a circle for a certain input polarization angle θ_1. The effect of any linear nondepolarizing optical system is to transform incident polarization states on a circle onto outgoing states on another circle.[11] Therefore we claim that a quarter-wave plate placed behind the liquid crystal display can project the set of polarization ellipses onto a meridian circle. This gives in a first approximation the desired solution. The complete optical setup is depicted in Fig. 6.

Next, we provide the mathematical foundation for the proposed approach. The output Jones vector, in the framework, is obtained by the matrix product,

$$\begin{pmatrix} E_x \\ E_y \end{pmatrix} = \exp(-i\beta)\mathbf{WP}\left(\frac{\pi}{2}, \theta_2\right)\mathbf{R}(\phi_{\mathrm{eq}})\mathbf{WP}\left(2\delta_{\mathrm{eq}}, \frac{\phi + \phi_{\mathrm{eq}}}{2}\right) \times \begin{pmatrix} \cos\theta_1 \\ \sin\theta_1 \end{pmatrix}, \tag{16}$$

where θ_2 is the orientation of the quarter-wave plate slow axis. Taking into account Eqs. (5) and (16), the Stokes parameters of the emerging light are given by

$$\begin{aligned} S_0 &= 1, \\ S_1 &= \cos(2\theta_2)(\cos^2\delta_{\mathrm{eq}}\cos[2(\theta_1 - \theta_2 - \phi_{\mathrm{eq}})] \\ &\quad + \sin^2\delta_{\mathrm{eq}}\cos[2(\theta_1 + \theta_2 - \phi)]) \\ &\quad + \sin(2\theta_2)\sin(2\delta_{\mathrm{eq}})\sin[2\theta_1 - \phi - \phi_{\mathrm{eq}}], \\ S_2 &= \sin(2\theta_2)(\cos^2\delta_{\mathrm{eq}}\cos[2(\theta_1 - \theta_2 - \phi_{\mathrm{eq}})] \\ &\quad + \sin^2\delta_{\mathrm{eq}}\cos[2(\theta_1 + \theta_2 - \phi)]) \\ &\quad - \cos(2\theta_2)\sin(2\delta_{\mathrm{eq}})\sin[2\theta_1 - \phi - \phi_{\mathrm{eq}}], \\ S_3 &= -\sin^2\delta_{\mathrm{eq}}\sin[2(\theta_1 + \theta_2 - \phi)] \\ &\quad + \cos^2\delta_{\mathrm{eq}}\sin[2(\theta_1 - \theta_2 - \phi_{\mathrm{eq}})]. \end{aligned} \tag{17}$$

The azimuth α of the final polarization state can be derived through Eq. (10) from the Stokes parameters S_1 and S_2. Note that for each addressed gray level g, i.e., for each value of the pair $(\delta_{\mathrm{eq}}, \phi_{\mathrm{eq}})$, the mathematical expressions for S_1 and S_2 become functions of two variables, namely, θ_1 and θ_2. Our task is to find the values for θ_1 and θ_2 which lead to a constant azimuth angle independent of the g value. For this purpose, a least-square procedure is outlined to determine the values of θ_1 and θ_2 that minimize the standard deviation σ defined as

$$\sigma(\theta_1, \theta_2) = \sqrt{\frac{1}{n-1}\sum_g (\alpha_g - \bar{\alpha})^2}. \tag{18}$$

In the above equation, $\bar{\alpha}$ is the mean value of the azimuth and n is the number of addressed gray levels.

The numerical simulation was performed with the aid of commercially available software. The variables θ_1 and θ_2 ranged from 0 to 180 in two-unit steps. The resulting angles for the axes of the polarizer and the quarter-wave plate are $\theta_1 = -28°$ and $\theta_2 = 16°$, for which the azimuth mean value is $\bar{\alpha} = -0.65°$ with a standard deviation $\sigma = 1.5°$. The small value of σ points out that the TNLCD can generate, in a first approximation, a set of EAPSs. The procedure was experimentally tested by measuring the Stokes parameters of the light emerging from the quarter-wave plate in Fig. 6. Figure

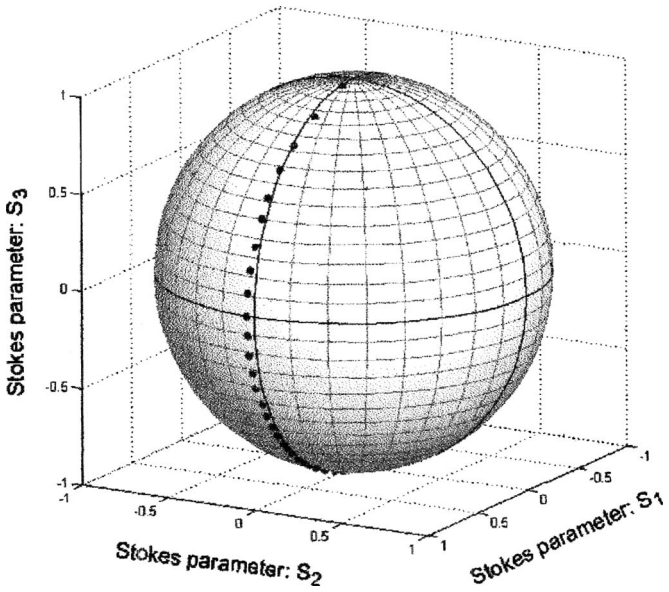

FIG. 8. Representation on the Poincaré sphere of the output polarization states in the configuration that provides a set of EAPSs.

7 shows the projection of the final polarization states over the S_1-S_2 plane. As expected, there is a linear relation between S_1 and S_2, since the projection of a meridian line in the Poincaré equatorial plane is a straight line that passes through the origin. By means of the least-square fit, we find that $S_2=-0.0685S_1+0.0323$. The linear correlation coefficient is $r=0.9052$. Assuming that the independent coefficient of the fit is negligible, the mean value of the azimuth can be derived from the slope of the curve, giving $\bar{\alpha}=-1.96°$. This result agrees reasonably well with the theoretical value. Finally, Fig. 8 shows the representation of the output polarization states on the Poincaré sphere. Note that the EAPSs approximately describe a semicircle onto the Poincaré sphere between the points R, right circularly polarized light, and L, left circularly polarized light.

IV. CONCLUSIONS

We have presented an original method for the calibration of an on-state TNLCD based on the equivalence between a liquid crystal cell and an optical system that consists of a phase retarder followed by a rotator. In contrast to previous calibration procedures we have demonstrated that the physical parameters of the equivalent system can be determined with an easily implemented device integrated by commercially available elements. Experimental calibration curves for a commercial display have been reported. The retarder-rotator approach allows us to describe the action of the liquid crystal cell by two consecutive rotations on the Poincaré sphere. This geometrical description offers a unique tool for the engineering of the light-modulation capabilities of a TNLCD. In particular, we have designed an LCD-based EAPS generator. Applications of the device in the field of coherent optical signal processing will be the subject of further research.

ACKNOWLEDGMENTS

This research was funded by the Dirección General de Investigación Científica y Técnica, Spain, under Project No. FIS2004-02404. We also acknowledge the financial support from the Generalitat Valenciana (Grant Nos. GV04B18 and GV05/110).

[1] D. W. Berreman, Appl. Phys. Lett. **25**, 12 (1974).
[2] K. Lu and B. E. A. Saleh, Opt. Eng. (Bellingham) **29**, 240 (1990).
[3] J. A. Coy, M. Zaldarriaga, D. F. Grosz, and O. E. Martínez, Opt. Eng. (Bellingham) **35**, 15 (1996).
[4] A. Marquez, C. Iemmi, I. Moreno, J. A. Davis, J. Campos, and M. J. Yzuel, Opt. Eng. (Bellingham) **40**, 2558 (2001).
[5] I. Moreno, P. Velásquez, C. R. Fernández-Pousa, M. M. Sánchez-López, and F. Mateos, J. Appl. Phys. **94**, 3697 (2003).
[6] H. Hurwitz and R. C. Jones, J. Opt. Soc. Am. **31**, 493 (1941).
[7] S. T. Tang and H. S. Kwok, J. Opt. Soc. Am. A **18**, 2138 (2001).
[8] S. Stallinga, J. Appl. Phys. **86**, 4756 (1999).
[9] S. T. Tang and H. S. Kwok, J. Appl. Phys. **91**, 8950 (2002).
[10] V. Duran, J. Lancis, E. Tajahuerce, and Z. Jaroszewicz, J. Appl. Phys. **97**, 043101 (2005).
[11] R. M. A. Azzam and N. M. Bashara, *Ellipsometry and Polarized Light*, 1st ed. (Elsevier, Amsterdam, 1987), Chap. 1.
[12] M. R. Dennis, Opt. Commun. **213**, 201 (2002).
[13] O. V. Angelsky, I. I. Mokhun, A. I. Mokhun, and M. S. Soskin, Phys. Rev. E **65**, 036602 (2002).
[14] V. Duran, J. Lancis, E. Tajahuerce, and M. Fernández, Opt. Express (submitted).
[15] C. Soutar and K. Lu, Opt. Eng. (Bellingham) **33**, 2704 (1994).
[16] S. Huard, *Polarization of Light*, 1st ed. (Wiley, New York, 1997), Chap. 1, p. 23.
[17] P. R. Bevington and D. K. Robinson, *Data Reduction and Error Analysis for the Physical Sciences*, 2nd ed. (McGraw-Hill, Singapore, 1992), Chap. 3, p. 38.
[18] J. E. Bigelow and R. A. Kashnow, Appl. Opt. **16**, 2090 (1977).